Ladderlike Oligomers; Intramolecular Hydrogen Bonding, Push–Pull Character, and Electron Affinity

Koen Pieterse,[a] Jef A. J. M. Vekemans,[a] Huub Kooijman,[b] Anthony L. Spek,[b] and E. W. Meijer*[a]

Abstract: Symmetrical 2,5-bis(2-aminophenyl)pyrazines have been synthesized by application of the Stille coupling strategy. These cotrimers feature three important properties, namely strong intramolecular hydrogen bonding, push-pull character, and high electron affinity. The presence of intramolecular hydrogen bonds has been confirmed by ^{1}H NMR, IR spectroscopy, and single-crystal X-ray diffraction. The hydrogen bond strength can be increased by substituting the amino groups with stronger electron-withdrawing functionalities. Despite the anticipated enhanced π-conjugation through planarization, a hypsochromic shift was observed in the UV/Vis spectra, explained by a decrease in push–pull character. The electron affinity of the cotrimers was deduced from the first reduction potentials measured by cyclic voltammetry and is related to the electron-withdrawing character of the amino substituents. The results obtained have been compared with those of the corresponding 4-aminophenyl analogues and show that intramolecular hydrogen bonds can be used to design polymers with enhanced π conjugation as well as a high electron affinity.

Keywords: conjugation · donor–acceptor systems · electron-deficient compounds · hydrogen bonds · oligomers

Introduction

π-Conjugated polymers represent an attractive class of materials for application in electronic devices, since their ease of modification allows tuning of their optical and electronic properties. Since the discovery of electronic conductivity in doped π-conjugated polymers in the late 1970s,[1–3] research has mainly focused on *p*-type materials. To widen the scope of organic electronics, stable *n*-type doped π-conjugated materials are desirable.[4, 5] The field of organic *n*-type materials is, however, still underdeveloped and most *n*-type materials lack the stability and processability of their *p*-type counterparts.

Azaheterocycles have been shown to be appropriate building blocks for polymeric *n*-type materials due to their electron-deficient nature.[6] To guarantee reducibility and processability, the azaheterocycles in the polymer backbone have to be provided with solubilizing side groups without introducing steric interactions that would compromise the π conjugation. Tour et al. [7–10] described the synthesis of ladder-type polyazaheterocycles based on pyridine and on pyrazine, which are highly functionalized but still coplanar due to the presence of covalent linkages between adjacent aromatic rings. Instead of using covalent bonds, secondary interactions, such as hydrogen bonds, can be used to planarize a polymeric backbone.[11–15] In our group Delnoye et al.[12] synthesized a copolymer composed of alternating pyrazine and acylated 1,4-phenylenediamine units (Scheme 1), taking advantage of the hydrogen bond accepting capabilities of the pyrazine units to organize the system in a close to planar conformation.

Although this polymer incorporates electron-releasing phenylenediamine units in its π-conjugated backbone, it has

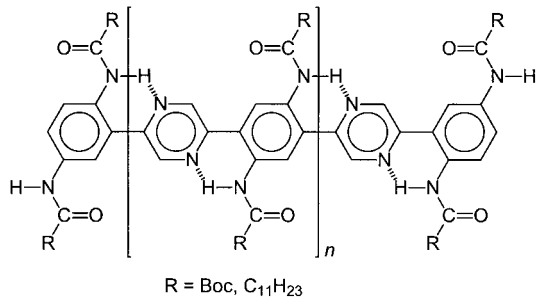

R = Boc, $C_{11}H_{23}$

Scheme 1. A copolymer composed of alternating pyrazine and acylated 1,4-phenylenediamine units.[12]

[a] Prof. E. W. Meijer, K. Pieterse, Dr. J. A. J. M. Vekemans
Laboratory of Macromolecular and Organic Chemistry
Eindhoven University of Technology
P. O. Box 513, 5600 MB Eindhoven (The Netherlands)
Fax: (+31) 40-2451036
E-mail: e.w.meijer@tue.nl

[b] Dr. H. Kooijman, Dr. A. L. Spek
Bijvoet Center for Biomolecular Research
Crystal and Structural Chemistry, Utrecht University
Padualaan 8, 3584 CH Utrecht (The Netherlands)
Fax: (+31) 30-2533940
E-mail: a.l.spek@chem.uu.nl

  0947-6539/00/0624-4597 $ 17.50+.50/0

revealed a first reduction potential as low as −1.37 V (SCE, 0.1 M Bu_4NPF_6 in THF, 100 mV s^{-1}). To obtain more insight into the relations between the three important features of polymers like this, being intramolecular hydrogen bonding, push–pull character, and electron affinity, cotrimers **1a–c** and reference compounds **2a–c** and **3** have been investigated and the results are described here.

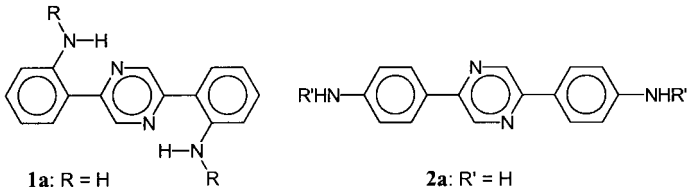

1a: R = H
1b: R = Boc
1c: R = $COCF_3$

2a: R' = H
2b: R' = Boc
2c: R' = $COCF_3$

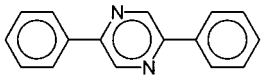

3

Results

Synthesis: The oligomers **1b**, **2b**, and **3** have all been synthesized by the Stille coupling methodology.[16, 17] Oligomers **1b** and **2b** have been prepared in 63 and 83% yield, respectively, both starting from 2,5-dibromopyrazine and *tert*-butoxycarbonyl (Boc) protected trimethylstannylaniline using $[Pd(PPh_3)_2Cl_2]$ as the catalyst and CuBr as the cocatalyst (Scheme 2). Due to the low solubility of oligomer **2b** in the solvent used (THF), **2b** can be collected as a solid material after the reaction without the need for further column chromatographic purifications. Oligomer **3** is synthesized in a 41% yield using a different catalytic system, namely $[Pd(PPh_3)_4]$ in a mixture of toluene and aqueous Na_2CO_3 (Scheme 2). As a result of the low reaction rate in this system, methyl transfer occurs during the reaction leading to formation of 2-methyl-5-phenylpyrazine as a side product.

Parent oligomers **1a** and **2a** have been prepared starting from oligomers **1b** and **2b** in 94 and 93% yield, respectively, by removal of the Boc-protecting groups by acidification with trifluoroacetic acid. Oligomers **1c** and **2c** have been prepared in 83 and 77% yield, respectively, by dissolving their corresponding Boc-protected analogues **1b** and **2b** in trifluoroacetic acid (leading to in situ deprotection), followed by acylation with trifluoroacetic anhydride.

Characterization: The oligomers obtained have been fully characterized by ^{1}H NMR, ^{13}C NMR, UV/Vis, and fluorescence spectroscopy and cyclic voltammetry (CV), while IR spectroscopy has been performed on the solid phase. Furthermore, single-crystal X-ray diffraction has been used to characterize cotrimers **1a–c** and **3**.

In ^{1}H NMR spectra the N–H signals are of special interest, since they can reveal the quality of hydrogen bonding in the oligomers provided with amino groups. The N–H signals belonging to the Boc-protected oligomers **1b** and **2b** show a strong downfield shift (4.8 and 2.7 ppm, respectively) in comparison to the signal of the amino-substituted oligomers **1a** and **2a**, but the strongest downfield shifts have been observed for the trifluoroacetyl derivatives **1c** and **2c** (Table 1). Furthermore, the N-H signals of the oligomers substituted at the *para* positions of the phenyl rings (**2a–c**) have been found considerably upfield compared to those of their corresponding *ortho*-substituted derivatives **1a–c**.

Table 1. Physical data on the cotrimers in solution.

Oligomer	^{1}H NMR[a] δ_{N-H} [ppm]	UV/Vis[b] λ_{max} [nm]	Fluorescence[b] λ_{max} [nm]	CV[c] E_{pc} [V]
1a	5.71	387	437	−2.00
1b	10.52	359	409	−1.70
1c	13.13	353	395	−1.26/−1.58
2a	3.89	367	446	< −2.30
2b	6.60	352	414	−1.96
2c	11.48[d]	342	395	−1.71/−1.91
3	–	324	374	−2.03

[a] Measured in deuterated chloroform. [b] Measured in chloroform. [c] CV conditions: THF, 0.1 M Bu_4NPF_6, SCE, 100 mV s^{-1}. [d] Oligomer **2c** was measured in $[D_6]$DMSO due to poor solubility in deuterated chloroform.

UV/Vis spectroscopic data on the oligomers showed a hypsochromic shift of the λ_{max} value of the acylated oligomers compared to their parent amino derivatives (Figure 1). The *para*-substituted oligomers are hypsochromic in comparison with the *ortho*-substituted compounds. In addition, the λ_{max} of the fluorescence measurements follows the trend that was observed for the λ_{max} of the UV/Vis spectra, exhibiting Stokes shifts ranging from 42 nm up to 79 nm. The intensity of the fluorescence is, however, almost two orders of magnitude lower for the *ortho*-substituted oligomers than for the *para*-substituted ones (Figure 2).

To establish the electron affinity of the synthesized cotrimers, first reduction poten-

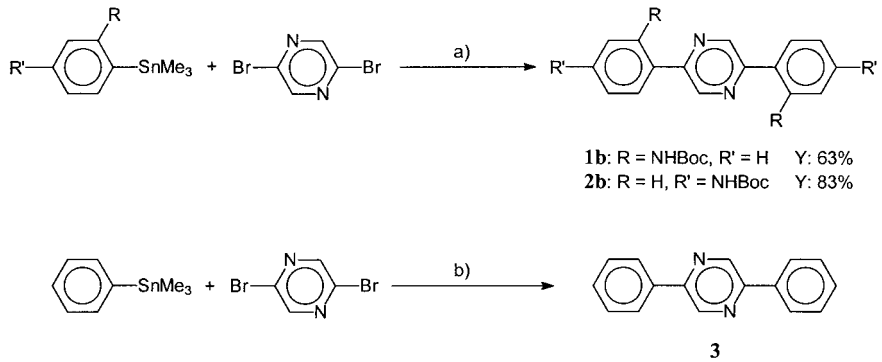

1b: R = NHBoc, R' = H Y: 63%
2b: R = H, R' = NHBoc Y: 83%

3

Scheme 2. Synthesis of oligomers **1b**, **2b** and **3**. a) $[Pd(PPh_3)_2Cl_2]$, CuBr, THF; b) $[Pd(PPh_3)_4]$, toluene, 0.5 M Na_2CO_3, 41%.

0947-6539/00/0624-4598 $ 17.50+.50/0 *Chem. Eur. J.* **2000**, *6*, No. 24

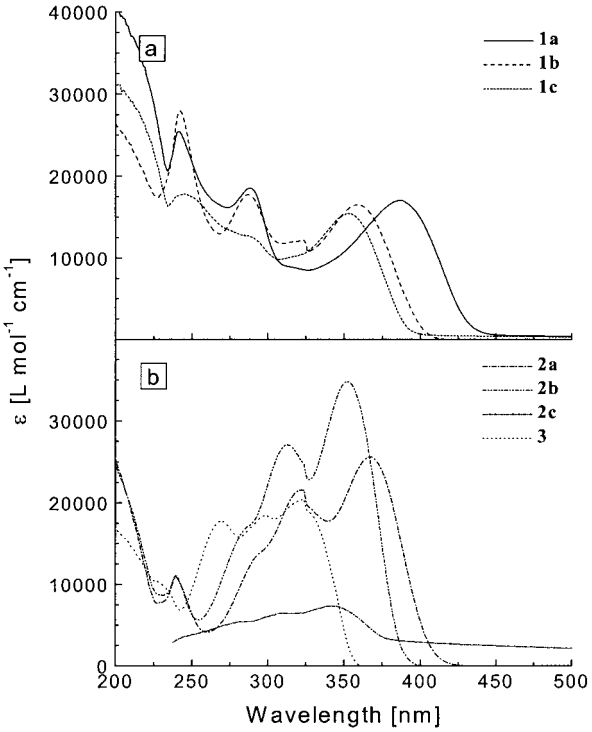

Figure 1. UV/Vis spectra of oligomers a) **1a–c** and b) **2a–c**, and **3** in chloroform.

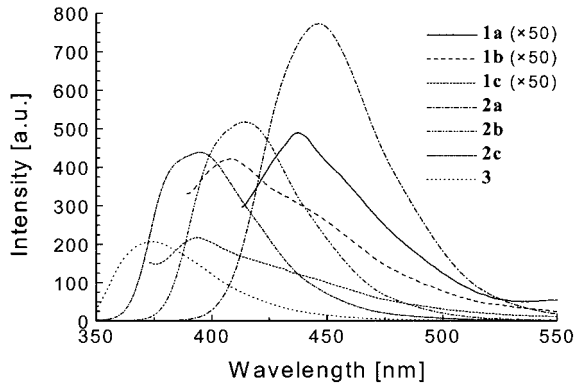

Figure 2. Fluorescence spectra of oligomers **1a-c**, **2a–c**, and **3** in chloroform.

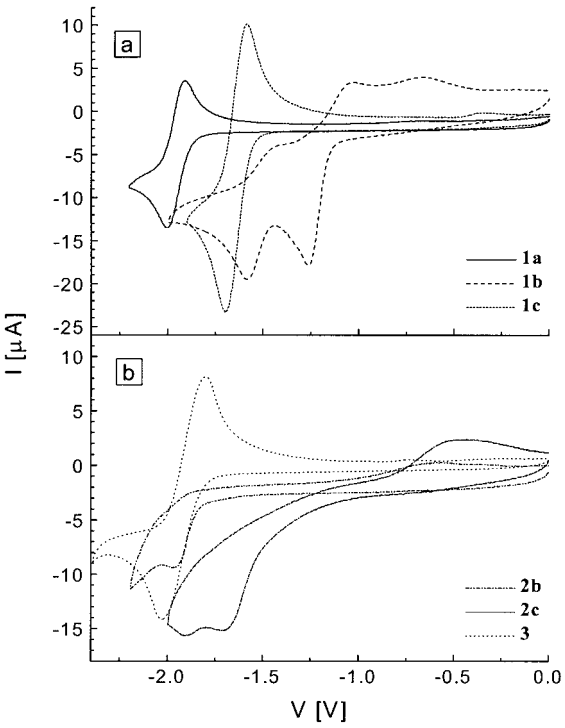

Figure 3. Cyclic voltammograms of oligomers a) **1a–c** and b) **2a–c** and **3**.

Table 2. Physical data on the cotrimers in solid phase.

Oligomer	IR[a] $\tilde{\nu}_{N-H}$ [cm^{-1}]	Single-crystal X-ray diffraction: H···N[b] [Å]	N···N[c] [Å]	N–H···N[d] [°]	Interplane angle[e] [°]
1a	3465, 3359	2.106(15)	2.7795(15)	128.4(16)	31.17(5)
1b	3253	2.035(5)	2.697(7)	131.3(3)	21.4(3)
		2.039(5)	2.708(7)	132.0(3)	20.0(3)
1c	2891	1.88(2)	2.6314(17)	141.9(17)	15.16(6)
2a	3423, 3305, 3184	–	–	–	–
2b	3358	–	–	–	–
2c	3321	–	–	–	–
3	–	–	–	–	20.92(15)

[a] Measured by ATR. [b] Distance between the N-H proton and the pyrazine nitrogen. [c] Distance between the N-H nitrogen and the pyrazine nitrogen. [d] Bond angle between the N–H bond and the hydrogen bond. [e] Angle between the planes through the pyrazine and phenyl rings.

tials have been measured by cyclic voltammetry (Figure 3). With respect to the parent amino compounds, lower first reduction potentials have been found for the acylated oligomers (Table 1). Furthermore, it is possible to reduce the trifluoroacetyl functionalized cotrimers twice. Again a significant difference is observed between the *ortho*- and *para*-substituted oligomers; the latter feature much higher first reduction potentials.

Besides in solutions, the properties of the cotrimers in the solid phase have also been investigated. IR spectra show that N–H stretch vibrations shift to lower wavenumbers upon acylation of the amino oligomers (Table 2), especially in the *ortho* series. From oligomers **1a–c** and **3** sufficiently large crystals have been obtained to determine their crystal structures by single-crystal X-ray diffraction. In Table 2 typical distances and angles (standard deviation in parentheses) are given. The smallest absolute torsion angle between the phenyl rings and the central pyrazine ring was found for the trifluoroacetyl derivatized oligomer **1c**, while amino oligomer **1a** deviated most from coplanarity (Figure 4).

Discussion

One of the important features of cotrimers **1a–c** is their ability to form intramolecular hydrogen bonds. In the solid phase the presence of intramolecular hydrogen bonds has been confirmed by the crystal structures, which show hydrogen bond lengths of approximately 2.7 Å. Furthermore, bistrifluoroacetyl oligomer **1c** features additional intramolecular contact between the N-H proton and one of the fluorine atoms of the CF_3 group. The interplane angle between the planes through the phenyl rings and the central pyrazine ring

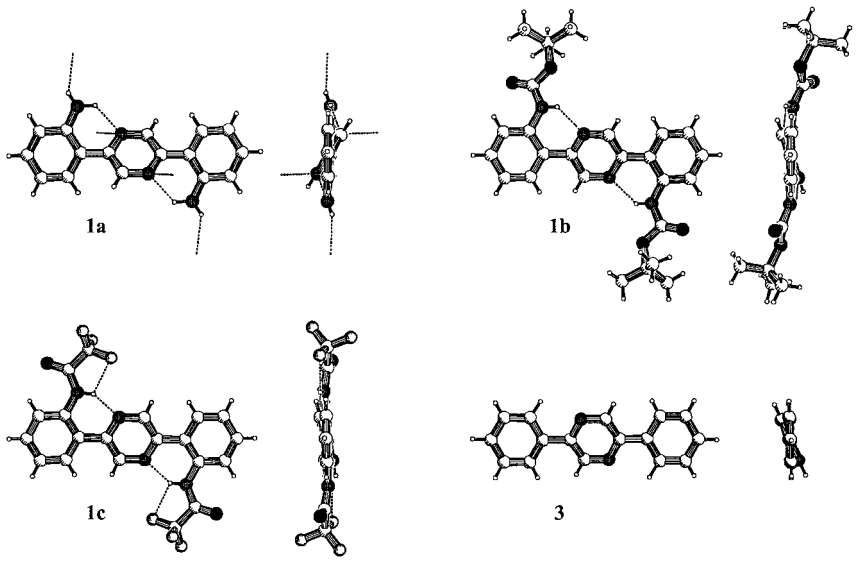

Figure 4. PLUTON representations showing the front and side views of the crystal structures of oligomers **1a–c** and **3**.

decreases by incorporation of an electron-withdrawing group. Although this might be due to an increase in hydrogen bond strength, crystal packing effects can not be excluded.

Another indication for hydrogen bonding was found in the IR spectra. Compounds **1b** and **1c** show N–H stretch vibrations at lower wavenumbers and feature broader signals in comparison with **2b** and **2c** (Table 2). Surprisingly, cotrimer **2a** features three N–H stretch vibrations. The two signals at higher wavenumbers can be attributed to the free amino group; however, the signal at 3184 cm^{-1} suggests the presence of a hydrogen-bonded N-H proton. Evidently, an intermolecular hydrogen bond seems likely.

^{1}H NMR data in deuterated chloroform show that the N–H signals belonging to cotrimers **1a–c** are shifted downfield in comparison with those of cotrimers **2a–c**. This implies that intramolecular hydrogen bonding in the *ortho*-substituted compounds, which is observed in the solid phase, is also present in solution. Derivatizing the amino groups in compound **1a** and **2a** with the electron-withdrawing Boc or trifluoroacetyl groups, strongly shifts the N–H signals downfield. The enhanced acidity of the N-H proton in the case of cotrimers **1a–c**, leads to increased hydrogen bond strength.

Since ^{1}H NMR data have shown the occurrence of intramolecular hydrogen bonding in cotrimers **1a–c**, the influence of these secondary interactions on the optical properties of the synthesized oligomers in chloroform has been investigated by UV/Vis and fluorescence spectroscopy. When one proton of the amino groups in cotrimer **1a** is replaced by electron-withdrawing groups, one might expect a bathochromic shift of the λ_{max} values in the UV/Vis spectra, since the increase in hydrogen bonding strength will lead to a more planar cotrimer (as was shown in single crystals) and thus enhanced π conjugation. The fact that a hypsochromic shift is observed (Table 1), can be attributed to counteracting push–pull effects in the cotrimers, in which the electron-releasing phenyl rings act as donors, while the electron-deficient pyrazine ring behaves as the acceptor. Substituting stronger electron-withdrawing groups on the amino groups of cotrimer **1a** will not only increase hydrogen-bond strength, but will concomitantly reduce the donor character of the phenyl rings, therefore, decreasing the overall push–pull character of the oligomers. As is apparent from the λ_{max} values in Table 1, the influence of the latter on the UV/Vis absorption of the oligomers surpasses the gain in π conjugation. A hypsochromic shift is also observed when comparing cotrimer **2a** with **2b** and **2c**. In addition, a large difference in fluorescence intensity exists between the *ortho*- and *para*-substituted oligomers. The rationale behind the quenching of the fluorescence by intramolecular hydrogen bonding in cotrimers **1a–c** is not yet clear, presumably the possibility for (double) intramolecular proton transfer and the rigidification of the cotrimer backbone enable energy dissipation by nonradiative pathways.

To investigate the electron affinity of the synthesized cotrimers, first reduction potentials have been measured by cyclic voltammetry in THF solutions. Table 1 shows lower first reduction potentials for cotrimers **1a–c** compared to those for references **2a–c**. This is attributed to the enhanced π conjugation in the former oligomers induced by the intramolecular hydrogen bonding. Furthermore, the first reduction potentials of parent oligomers **1a** and **2a** are lowered by substitution of the amino functionalities with electron-withdrawing groups. The decreased donor character of the phenyl rings increases the electron affinity of the π-conjugated system.

Conclusion

Herein we have shown that intramolecular hydrogen bonds are capable of planarizing π-conjugated systems and, at the same time, allow the introduction of solubilizing groups. The hydrogen-bond strength as well as the electron affinity can be increased in oligomers **1a–c** by placing more electron-withdrawing substituents on the amino groups. Since the intramolecular hydrogen bonds form spontaneously during the synthesis of the π-conjugated backbone and allow easy tuning of the properties of the synthesized structures, they form an attractive alternative for covalent linkages in ladder polymers. Although the electron affinities of the sythesized oligomers are nowhere near those of 2,3-chloro-5,6-dicyano-1,4-benzoquinone (DDQ), 7,7,8,8-tetracyano-*p*-quinodimethane (TCNQ), tetracyanoethylene (TCNE), etc., the results give basic insight into the properties of π-conjugated alternating polymers and will be used to design new *n*-type semiconducting polymers.

0947-6539/00/0624-4600 $ 17.50+.50/0 *Chem. Eur. J.* **2000**, *6*, No. 24

Experimental Section

General: All solvents used were p.a. quality. Tetrahydrofuran (THF) was distilled over Na/K/benzophenone. For column chromatography Merck silica gel 60 was used. Melting points were determined by using a Jenaval polarization microscope equipped with a Linkam THMS 600 heating device. ^{1}H NMR and ^{13}C NMR spectra were recorded on an AM-400 Bruker spectrometer with frequencies of 400.1 and 100.6 MHz, respectively. Chemical shifts are given in ppm (δ) downfield from tetramethylsilane (TMS). UV/Vis spectra were recorded on a Perkin Elmer Lambda 3B spectrophotometer or on a Perkin Elmer Lambda 900 UV/Vis/NIR spectrophotometer. Fluorescence spectra were recorded on a Perkin Elmer LS50B luminescence spectrometer and infrared spectra on a Perkin-Elmer Spectrum One using attenuated total reflection (ATR) sample accessory. Elemental analysis was performed on a Perkin Elmer 2400 series analyzer. Cyclic voltammograms were obtained in THF with 0.1M tetrabutylammonium hexafluorophosphate as supporting electrolyte using a Potentioscan Wenking POS73 potentiostat. A platinum disk (diameter 5 mm) was used as working electrode, the counter electrode was a platinum plate (5×5 mm^2) and a saturated calomel electrode (SCE) was used as reference electrode.

2,5-Bis(2′-aminophenyl)pyrazine (1a): 2,5-Bis(2′-*tert*-butoxycarbonylaminophenyl)pyrazine (**1b**, 0.14 g, 0.30 mmol) was dissolved in a solution of trifluoroacetic acid (5 mL) and dichloromethane (5 mL). The solution was briefly heated to 60 °C and subsequently neutralized with a saturated Na_2CO_3 solution in water. The two phases were separated and the water layer was extracted with another portion of dichloromethane. The combined organic layers were then washed with water, dried over $MgSO_4$, filtered, and evaporated to dryness. Column chromatography (SiO_2, ethyl acetate (2.5 %) in dichloromethane) of the crude material finally afforded **1a** as a yellow solid (0.0744 g, 0.284 mmol; 94 %). M. p. 225 °C; ^{1}H NMR (400 MHz, $CDCl_3$, 22 °C, TMS): $\delta = 8.93$ (s, 2H; H-3,6), 7.63 (dd, $J = 7.9$ and 1.4 Hz, 2H; H-3′), 7.22 (m, 2H; H-5′), 6.82 (t, $J = 7.6$ Hz, 2H; H-4′), 6.79 (dd, $J = 8.1$ and 0.6 Hz, 2H; H-6′), 5.71 (s, 4H; N-H); ^{13}C NMR (100 MHz, $CDCl_3$, 22 °C, TMS): $\delta = 151.0$, 147.1, 10.3, 130.7, 128.7, 118.6, 117.8, 117.4; IR (ATR): $\tilde{\nu} = 3465.1$, 3358.7, 1603.9, 1590.7, 1494.0, 1480.4, 1443.5, 1306.5, 1283.6, 1244.0, 1158.0, 1137.3, 1065.9, 1030.8, 1010.9, 915.1, 857.4, 751.9 cm^{-1}; UV/Vis ($CHCl_3$): λ_{max} (ε) = 387 nm (17 000 L mol^{-1} cm^{-1}); fluorescence ($CHCl_3$): $\lambda_{max} = 437$ nm; elemental analysis (%) for $C_{16}H_{14}N_4$ (262.31): calcd: C 73.26, H 5.38, N 21.36; found: C 73.08, H 5.36, N 20.73.

2,5-Bis(2′-*tert*-butoxycarbonylaminophenyl)pyrazine (1b):[12] Under continuous stirring, a solution of 2,5-dibromopyrazine (0.203 g, 0.86 mmol), *N*-(*tert*-butoxycarbonyl)-2-trimethylstannylaniline (0.626 g, 1.76 mmol) and CuBr (0.0110 g, 0.0766 mmol, 8.9 mol %) in THF (8 mL) was frozen using a liquid nitrogen bath and degassed to a pressure of 0.1 mbar. The solution was thawed and flushed with argon. This cycle was repeated before $[Pd(PPh_3)_2Cl_2]$ (0.0307 g, 0.0437 mmol, 5.1 mol %) was added. The freeze–thaw cycle was repeated five times and the solution was heated under reflux for 24 h. The solution was cooled, evaporated to dryness and subsequently dissolved in chloroform. The organic layer was then washed with an aqueous ethylenediamine solution (5 %), water ($3 \times$), and brine. After drying over $MgSO_4$, filtration, and evaporation of the solvent, the crude product was purified by column chromatography (SiO_2, hexane (10 %) in dichloromethane) yielding **1b** as a white solid (0.25 g, 0.54 mmol; 63 %). M. p. 234 °C (decomp); ^{1}H NMR (400 MHz, $CDCl_3$, 22 °C, TMS): $\delta = 10.50$ (s, 2H; N–H), 9.00 (s, 2H; H-3,6), 8.35 (d, $J = 8.2$ Hz, 2H; H-6′), 7.71 (dd, $J = 7.9$ and 1.5 Hz, 2H; H-3′), 7.45 (m, 2H; H-5′), 7.15 (td, $J = 7.8$ and 1.1 Hz, 2H; H-4′), 1.52 (s, 18H; Boc); ^{13}C NMR (100 MHz, $CDCl_3$, 22 °C, TMS): $\delta = 153.1$, 150.8, 141.4, 138.6, 130.9, 128.7, 122.6, 122.2, 120.9, 80.3, 28.3; IR (ATR): $\tilde{\nu} = 3252.6$, 2983.2, 1733.6, 1606.4, 1578.4, 1515.9, 1483.7, 1434.4, 1367.4, 1324.6, 1278.7, 1222.8, 1143.9, 1050.4, 1022.2, 832.1, 754.0, 717.0 cm^{-1}; UV/Vis ($CHCl_3$): λ_{max} (ε) = 359 nm (16 500 L mol^{-1} cm^{-1}); fluorescence ($CHCl_3$): $\lambda_{max} = 409$ nm; elemental analysis (%) for $C_{26}H_{30}N_4O_4$ (462.55): calcd: C 67.51, H 6.54, N 12.11; found: C 67.19, H 6.58, N 11.76.

2,5-Bis(2′-trifluoroacetylaminophenyl)pyrazine (1c): 2,5-Bis(2′-*tert*-butoxycarbonylaminophenyl)pyrazine (**1b**, 0.0072 g, 0.016 mmol) was dissolved in trifluoroacetic acid (1 mL), and trifluoroacetic anhydride (0.20 mL) was slowly added. The solution was stirred at room temperature for 45 min and then water (2 mL) was added. The precipitated solid was collected, washed with water and dried in a vacuum stove at 60 °C, affording **1c** as an off-white solid (0.0059 g, 0.013 mmol; 83 %). M. p. 282 °C; ^{1}H NMR (400 MHz, $CDCl_3$, 22 °C, TMS): $\delta = 13.13$ (s, 2H; N-H), 9.14 (s, 2H; H-3,6), 8.64 (d, $J = 8.4$ Hz, 2H; H-6′), 7.95 (dd, $J = 7.9$ and 1.3 Hz, 2H; H-3′), 7.59 (m, 2H; H-5′), 7.40 (m, 2H; H-4′); ^{13}C NMR (100 MHz, $CDCl_3$, 22 °C, TMS): $\delta =$ 155.0 (q, $J_{C,F} = 38$ Hz), 150.4, 140.2, 136.2, 132.0, 128.4, 125.8, 122.5, 122.1, 116.0 (q, $J_{C,F} = 289$ Hz); IR (ATR): $\tilde{\nu} = 2890.8$, 1714.6, 1608.5, 1588.6, 1549.4, 1445.7, 1341.6, 1272.3, 1171.2, 1148.1, 1117.4, 1051.2, 1018.1, 894.0, 769.3, 752.6, 739.9, 685.7 cm^{-1}; UV/Vis ($CHCl_3$): λ_{max} (ε) = 353 nm (15 400 L mol^{-1} cm^{-1}); fluorescence ($CHCl_3$): $\lambda_{max} = 395$ nm; elemental analysis (%) for $C_{20}H_{12}F_6N_4O_2$ (454.33): calcd: C 52.87, H 2.66, N 12.33; found: C 52.98, H 2.73, N 11.81.

2,5-Bis(4′-aminophenyl)pyrazine (2a): 2,5-Bis(4′-*tert*-butoxycarbonylaminophenyl)pyrazine (**2b**, 0.20 g, 0.43 mmol) was dissolved in a solution of trifluoroacetic acid (5 mL) and dichloromethane (10 mL). The solution was briefly heated to 60 °C and subsequently neutralized with a saturated Na_2CO_3 solution in water. The precipitated solid was collected, washed with water and dichloromethane and dried in a vacuum stove at 50 °C, affording **2a** as a yellow solid (0.106 g, 0.404 mmol; 93 %). M. p. 280 °C (decomp); ^{1}H NMR (400 MHz, $CDCl_3$, 22 °C, TMS): $\delta = 8.90$ (s, 2H; H-3,6), 7.87 (d, $J = 8.7$ Hz, 4H; H-2′,6′), 6.80 (d, $J = 8.6$ Hz, 4H; H-3′,5′), 3.89 (s, 4H; N-H); ^{13}C NMR (100 MHz, [D$_6$]DMSO, 22 °C, TMS): $\delta =$ 150.3, 148.4, 139.1, 127.2, 123.3, 113.9; IR (ATR): $\tilde{\nu} = 3423.2$, 3305.2, 3183.7, 1635.7, 1599.2, 1474.7, 1438.0, 1350.0, 1293.9, 1176.0, 1155.8, 1130.6, 1024.8, 827.5 cm^{-1}; UV/Vis ($CHCl_3$): λ_{max} (ε) = 367 nm (25 600 L mol^{-1} cm^{-1}); fluorescence ($CHCl_3$): $\lambda_{max} = 446$ nm.

2,5-Bis(4′-*tert*-butoxycarbonylaminophenyl)pyrazine (2b): Under continuous stirring, a solution of 2,5-dibromopyrazine (0.685 g, 2.88 mmol), *N*-(*tert*-butoxycarbonyl)-4-trimethylstannylaniline (2.40 g, 6.74 mmol) and CuBr (0.0351 g, 0.245 mmol, 8.5 mol %) in THF (26 mL) was frozen using a liquid nitrogen bath and degassed to a pressure of 0.1 mbar. The solution was thawed and flushed with argon. This cycle was repeated before $[Pd(PPh_3)_2Cl_2]$ (0.0850 g, 0.121 mmol, 4.2 mol %) was added. The freeze–thaw cycle was repeated four times and the solution was heated under reflux for three days. The mixture was cooled, the solid collected and washed with THF and diethyl ether yielding **2b** as a white solid (1.10 g, 2.38 mmol; 83 %). M. p. >300 °C (decomp); ^{1}H NMR (400 MHz, $CDCl_3$, 22 °C, TMS): $\delta = 9.00$ (s, 2H; H-3,6), 8.01 (dd, $J = 6.8$ and 1.9 Hz, 4H; H-2′,6′), 7.52 (d, $J = 8.7$ Hz, 4H; H-3′,5′), 6.60 (s, 2H; N-H), 1.54 (s, 18H; Boc); ^{13}C NMR (100 MHz, [D$_6$]DMSO, 22 °C, TMS): $\delta = 152.6$, 148.7, 141.1, 140.3, 129.3, 126.9, 118.2, 79.4, 28.1; IR (ATR): $\tilde{\nu} = 3358.1$, 1698.3, 1533.4, 1504.6, 1472.8, 1414.8, 1367.8, 1305.8, 1251.8, 1230.1, 1156.3, 1068.8, 1054.3, 1017.6, 834.9, 771.6 cm^{-1}; UV/Vis ($CHCl_3$): λ_{max} (ε) = 352 nm (34 800 L mol^{-1} cm^{-1}); fluorescence ($CHCl_3$): $\lambda_{max} = 414$ nm.

2,5-Bis(4′-trifluoroacetylaminophenyl)pyrazine (2c): 2,5-Bis(4′-*tert*-butoxycarbonylaminophenyl)pyrazine (**2b**, 0.100 g, 0.216 mmol) was dissolved in trifluoroacetic acid (3 mL), and trifluoroacetic anhydride (0.50 mL) was slowly added. The solution was stirred at room temperature for 45 min and then water (6 mL) was added. The precipitated solid was collected, washed with water and dried in a vacuum stove at 60 °C, affording **2c** as a pale-yellow solid (0.0753 g, 0.166 mmol; 77 %). M. p. >350 °C; ^{1}H NMR (400 MHz, [D$_6$]DMSO, 22 °C, TMS): $\delta = 11.48$ (s, 2H; N-H), 9.32 (s, 2H; H-3,6), 8.26 (d, $J = 8.7$ Hz, 4H; H-2′,6′), 7.88 (d, $J = 8.7$ Hz, 4H; H-3′,5′); IR (ATR): $\tilde{\nu} = 3320.8$, 1697.9, 1597.2, 1539.9, 1477.2, 1420.1, 1344.0, 1291.0, 1171.2, 1146.8, 1112.2, 1068.3, 1012.2, 906.6, 829.5, 742.5, 683.3, 668.5 cm^{-1}; UV/Vis ($CHCl_3$): λ_{max} (ε) = 342 nm (7400 L mol^{-1} cm^{-1}); fluorescence ($CHCl_3$): $\lambda_{max} = 395$ nm; elemental analysis (%) for $C_{20}H_{12}F_6N_4O_2$ (454.33): calcd: C 52.87, H 2.66, N 12.33; found: C 52.66, H 2.74, N 12.12.

2,5-Diphenylpyrazine (3):[18] A solution of 2,5-dibromopyrazine (0.47 g, 1.98 mmol) and trimethylstannylbenzene (1.23 g, 5.11 mmol) in toluene (10 mL) and aqueous Na_2CO_3 (0.5M, 20 mL) was deaerated and stored under argon. $[Pd(PPh_3)_4]$ (0.0241 g, 0.0209 mmol, 1.1 mol %) was added, and the reaction mixture was heated under reflux for three days. After this period, water (50 mL) and dichloromethane (30 mL) were added, the two layers were separated, and the aqueous layer was extracted twice with dichloromethane (30 mL). The combined organic layers were then washed with water (2×50 mL) and brine (50 mL), dried over $MgSO_4$, filtered, and evaporated to dryness. Column chromatography (SiO_2, hexane (25 %) in dichloromethane) of the crude material yielded **3** as a white solid (0.19 g, 0.82 mmol; 41 %). M. p. 197 °C; ^{1}H NMR (400 MHz, $CDCl_3$, 22 °C, TMS): $\delta = 9.08$ (s, 2H; H-3,6), 8.07 (m, 4H; H-2′,6′), 7.56–7.46 (m, 6H; H-3′,4′,5′);

Table 3. Crystallographic data for **1a–c** and **3**.

Compound	**1a**	**1b**	**1c**	**3**
		Crystal data		
formula	$C_{16}H_{14}N_4$	$C_{26}H_{30}N_4O_4$	$C_{20}H_{12}F_6N_4O_2$	$C_{16}H_{12}N_2$
molecular weight	262.31	462.55	454.33	232.28
crystal system	monoclinic	orthorhombic	triclinic	monoclinic
space group	$P2_1/c$ (no. 14)	$Pca2_1$ (no. 29)	$P\bar{1}$ (no. 2)	$P2_1/c$ (no. 14)
a [Å]	6.8891(6)	15.940(3)	7.0555(11)	13.359(4)
b [Å]	12.7250(16)	5.937(3)	7.108(2)	5.7080(9)
c [Å]	7.4918(10)	25.268(3)	9.822(2)	7.506(4)
α [°]	–	–	108.67(2)	–
β [°]	107.997(10)	–	93.099(16)	93.82(2)
γ [°]	–	–	103.91(2)	–
V [Å^3]	624.63(13)	2391.3(13)	448.35(19)	571.1(4)
ρ_{calcd} [g cm^{-3}]	1.395	1.285	1.683	1.351
Z	2	4	1	2
$F(000)$	276	984	230	244
$\mu(Mo_{K\alpha})$ [mm^{-1}]	0.087	0.088	0.154	0.081
crystal size [mm]	$0.2\times0.2\times0.3$	$0.02\times0.6\times0.6$	$0.1\times0.3\times0.4$	$0.05\times0.1\times0.3$
crystal color	yellow	pale yellow	colorless	colorless
		Data collection		
θ_{min}, θ_{max} [°]	1.6, 27.5	0.8, 27.5	2.2, 27.5	1.5, 25.0
cell determination				
no. refl	25	25	19	19
θ range	10.05–15.59	9.71–13.56	9.99–14.01	7.03–16.82
$\Delta\omega$ [°]	$0.81+0.35\tan\theta$	$1.15+0.35\tan\theta$	$0.92+0.35\tan\theta$	$0.50+0.35\tan\theta$
X-ray exposure time [h]	25	13	14	14
data set	−8:8, −16:16, −9:9	−13:20, 0:7, 0:32	−9:8, −8:9, −12:12	−15:15, −6:0, −8:8
total data	4542	3968	4190	2068
total unique data	1429 [$R_{int}=0.0367$]	2796 [$R_{int}=0.0413$]	2057 [$R_{int}=0.0285$]	1003 [$R_{int}=0.1815$]
		Refinement		
no. of refined params	119	313	169	100
final R[a]	0.0365 [1262 $I>2\sigma(I)$]	0.0649 [1746 $I>2\sigma(I)$]	0.0325 [1802 $I>2\sigma(I)$]	0.0585 [631 $I>2\sigma(I)$]
final $wR2$[b]	0.0987	0.1621	0.0943	0.1478
goodness of fit	1.036	1.030	1.046	1.060
w^{-1}[c]	$\sigma^2(F^2)+(0.0524P)^2+0.17P$	$\sigma^2(F^2)+(0.0724P)^2+0.11P$	$\sigma^2(F^2)+(0.0506P)^2+0.12P$	$\sigma^2(F^2)+(0.0270P)^2+0.11P$
min. and max. residual density [e Å^{-3}]	−0.21, 0.23	−0.27, 0.24	−0.28, 0.34	−0.23, 0.20

[a] $R=\Sigma\,||F_o|-|F_c||/\Sigma|F_o|$. [b] $wR2=[\Sigma[w(F_o^2-F_c^2)^2]/\Sigma[w(F_o^2)^2]\,]^{1/2}$. [c] $P=(\mathrm{Max}(F_o^2,0)+2F_c^2)/3$.

^{13}C NMR (100 MHz, $CDCl_3$, 22 °C, TMS): $\delta=150.7$, 141.2, 136.3, 129.8, 129.1, 126.8; IR (ATR): $\tilde{\nu}=3060.7$, 1472.2, 1449.6, 1340.8, 1319.2, 1162.5, 1076.3, 1069.1, 1027.3, 1013.7, 909.1, 754.7, 685.8 cm^{-1}; UV/Vis ($CHCl_3$): λ_{max} (ε) = 324 nm (20400 L mol^{-1} cm^{-1}); fluorescence ($CHCl_3$): $\lambda_{max}=374$ nm; elemental analysis (%) for $C_{20}H_{12}F_6N_4O_2$ (232.28): calcd: C 82.73, H 5.21, N 12.06; found: C 82.57, H 5.19, N 12.00.

X-ray structure determination of 1a–c and 3: Crystals suitable for X-ray diffraction were glued to the tip of a glass capillary and placed in the cold nitrogen stream on an Enraf-Nonius CAD4-T diffractometer on rotating anode. Accurate unit cell parameters and an orientation matrix were determined by least-squares fitting of the setting angles of a limited set of reflections (SET4-centered[19] on the CAD4). Reduced-cell calculations did not indicate higher lattice symmetry.[20] Crystal data and details of the data collection and refinement are collected in Table 3. All data were collected at 150 K in the ω scan mode using graphite-monochromated $Mo_{K\alpha}$ radiation ($\lambda=0.71073$ Å). Data were corrected for Lp effects and the observed linear instability of the periodically measured reference reflections, but not for absorption. The crystals of compounds **1c** and **3** turned out to be twinned; intensity data were collected on the major twin component. All structures were solved by automated direct methods (SHELXS86[21] for **3**; SHELXS97[22] for the other compounds. The structures were refined on F^2, using full-matrix least-squares techniques (SHELXL-97[23]). The hydrogen atoms of **1b** were included in the refinement at calculated positions, riding on their carrier atoms; hydrogen atoms of all other compounds were located on difference Fourier maps and their coordinates were included as parameters in the refinement. All non-hydrogen atoms were refined with anisotropic atomic displacement parameters. The hydrogen atoms of **1b** and **3** were refined with fixed isotropic displacement parameters related to the value of the equivalent isotropic displacement parameters of their carrier atoms; the isotropic displacement parameters of the hydrogen atoms of **1a** and **1c** were refined. All structures were refined till $(\Delta/\sigma)_{max}<0.001$. Due to the lack of significant anomalous scattering, the absolute structure of **1b** could not be determined (Flack $x=-2(3)$ in the final structure factor calculation[24]). Neutral atom scattering factors and anomalous dispersion corrections were taken from the *International Tables for Crystallography*.[25] Geometrical calculations and illustrations were performed with PLATON.[26] Crystallographic data (excluding structure factors) for the structures reported in this paper have been deposited with the Cambridge Crystallographic Data Centre as supplementary publication nos. CCDC 144486–144489. Copies of the data can be obtained free of charge on application to CCDC, 12 Union Road, Cambridge CB2 1EZ, UK (fax: (+44) 1223 336–033; e-mail: deposit@ccdc.cam.ac.uk).

Acknowledgement

The authors would like to thank the Netherlands Foundation for Chemical Research (SON/PPM) and the Council for Chemical Sciences of the Netherlands Organization for Scientific Research (CW-NWO) for their financial support.

[1] H. Shirakawa, E. J. Louis, A. G. MacDiarmid, C. K. Chiang, A. J. Heeger, *J. Chem. Soc. Chem. Commun.* **1977**, 578.
[2] C. K. Chiang, C. R. Fincher, Y. W. Park, A. J. Heeger, H. Shirakawa, E. J. Louis, S. C. Gau, A. G. MacDiarmid, *Phys. Rev. Lett.* **1977**, *39*, 1098.
[3] C. K. Chiang, Y. W. Park, A. J. Heeger, H. Shirakawa, E. J. Louis, A. G. MacDiarmid, *J. Chem. Phys.* **1978**, *69*, 5098.

  0947-6539/00/0624-4602 $ 17.50+.50/0

[4] D. M. de Leeuw, M. M. J. Simenon, A. R. Brown, R. E. F. Einerhand, *Synth. Met.* **1997**, *87*, 53.
[5] H. E. Katz, A. J. Lovinger, J. Johnson, C. Kloc, T. Siegrist, W. Li, Y.-Y. Lin, A. Dodabalapur, *Nature* **2000**, *404*, 478.
[6] T. Yamamoto, *J. Polym. Sci. Part A: Polym. Chem.* **1996**, *34*, 997.
[7] Y. Yao, J. J. S. Lamba, J. M. Tour, *J. Am. Chem. Soc.* **1998**, *120*, 2805.
[8] Y. Yao, Q. T. Zhang, J. M. Tour, *Macromolecules* **1998**, *31*, 8600.
[9] Y. Yao, J. M. Tour, *Macromolecules* **1999**, *32*, 2455.
[10] C. Y. Zhang, J. M. Tour, *J. Am. Chem. Soc.* **1999**, *121*, 8783.
[11] J. A. Osaheni, S. A. Jenekhe, A. Burns, G. Du, J. Joo, Z. Wang, A. J. Epstein, C.-S. Wang, *Macromolecules* **1992**, *25*, 5828.
[12] D. A. P. Delnoye, R. P. Sijbesma, J. A. J. M. Vekemans, E. W. Meijer, *J. Am. Chem. Soc.* **1996**, *118*, 8717.
[13] M. Moroni, J. Le Moigne, T. A. Pham, J.-Y. Bigot, *Macromolecules* **1997**, *30*, 1964.
[14] S. K. Pollack, Y. M. Hijji, B. Kgobane, *Macromolecules* **1997**, *30*, 6709.
[15] H. A. M. van Mullekom, J. A. J. M. Vekemans, E. W. Meijer, *Chem. Eur. J.* **1998**, *4*, 1235.
[16] J. K. Stille, *Angew. Chem.* **1986**, *98*, 504.
[17] V. Farina, G. P. Roth, *Adv. Met.-Org. Chem.* **1996**, *5*, 1.
[18] J. Armand, K. Chekir, J. Pinson, *Can. J. Chem.* **1974**, *52*, 3971.
[19] J. L. de Boer, A. J. M. Duisenberg, *Acta Crystallogr. Sect. A* **1984**, *40*, C-410.
[20] A. L. Spek, *J. Appl. Crystallogr.* **1988**, *21*, 578.
[21] G. M. Sheldrick, SHELXS-86, Program for Crystal Structure Determinations, University of Göttingen, **1986**.
[22] G. M. Sheldrick, SHELXS-97, Program for Crystal Structure Determinations, University of Göttingen, **1997**.
[23] G. M. Sheldrick, SHELXL-97, Program for Crystal Structure Refinement, University of Göttingen, **1997**.
[24] H. D. Flack, *Acta Crystallogr. Sect. A* **1983**, *39*, 876.
[25] *International Tables for Crystallography*, *Vol. C* (Ed.: A. J. C. Wilson), Kluwer, Dordrecht, **1992**.
[26] A. L. Spek, *Acta Crystallogr. Sect. A* **1990**, *46*, C-34.

Received: May 23, 2000 [F2509]